Experimental study by the inclination method of dynamic scattering accompanying Laue reflection of X-rays by single crystals containing microdefects

S. N. Voronkov, D. I. Piskunov, F. N. Chukhovskiĭ, and S. K. Maksimov

Moscow Institute of Electronics Engineering
(Submitted 1 October 1986)
Zh. Eksp. Teor. Fiz. **92**, 1099–1109 (March 1987)

Dynamic scattering of x-rays in silicon crystals with randomly distributed structural defects is investigated experimentally and theoretically for a noncoplanar Laue diffraction. It is shown that the static Debye-Waller factor E and the correlation length τ for the random elastic displacements of the atoms in the crystal lattice can be deduced from x-ray diffraction measurements of the mean Laue reflection coefficient R_h as a function of the inclination angle α of the diffraction plane. A simple model is proposed, in which the crystal microdefects are assumed to be uniformly distributed spherical inclusions, and formulas are derived which relate E and τ to the concentration c and mean size r_0 of the microdefects. Measurements of $R_h(\alpha)$ are reported for silicon crystals with oxygen concentrations 10^{16}–10^{18} cm^{-3}, and the results are used to calculate c and r_0.

INTRODUCTION

The X-ray Bloch waves that form in crystals during dynamic scattering (diffraction and reflection) are highly sensitive to local disruptions in the periodicity of the crystal lattice. This is because small local distortions of magnitude comparable to the dielectric susceptibility ($\sim 10^{-5}$–10^{-6}) substantially alter the dynamic diffraction parameters by preventing coherent interference between the plane-wave components of the Bloch wave in the crystal. X-ray diffraction measurements of the diffraction parameters can reveal the distribution, type, and concentration of local crystal lattice defects such as clusters, dislocation loops, precipitates, and other microdefects. Studies of dynamic X-ray scattering (DXS) in crystals containing microdefects are also of considerable applied as well as theoretical interest, because microdefects are associated with local variations in the electrophysical properties of semiconductors (they can distort the band structure, produce additional levels in the forbidden band, and cause the minority carrier lifetime and the specific resistance to change locally).

The early experimental work[1–4] on DXS by microdefects considered the special case of anomalous transimission (Borrmann effect) in strongly absorbing crystals. The nature of the defects (whether they are primarily clusters or dislocations, for example) can be ascertained and their mean size r_0 and concentration c can be estimated in the range $r_0 = 10^2$–10^4 nm, $c = 10^{15}$–10^{18} c^{-3} by determining the X-ray interference absorption coefficient from the dependence of the average Laue reflection intensity on the thickness of the crystal.

In Refs. 5–10, a technique based on three-crystal X-ray diffractometry was developed for analyzing DXS in crystals with microdefects. This method makes it possible to distinguish (in reciprocal space) the diffuse and coherent components of the Bragg-reflected radiation from the crystal. The general theory for the formation and interpretation of angular reflection patterns and their relationship to defect structure is discussed in Refs. 9 and 10. However, because the diffusely scattered component is much weaker than the coherently scattered radiation, it is possible to reliably detect relatively large defects $r_0 \sim 10^4$ nm such as those generated when the crystal is annealed in an oxidizing atmosphere, decorated with impurity, etc.

An experimental method was developed in Ref. 11 for solving the inverse DXS scattering problem by measuring the elastic strain distribution in crystal plates. It involves measuring the mean Laue reflection intensity as a function of the inclination angle α of the diffraction plane about an axis normal to the reflecting plane. A least-squares analysis is then preformed to deduce the deformation gradient $B(\alpha)$ in accordance with the theory developed in Ref. 12. The first results on DXS obtained by this method for crystals with microdefects revealed that the angular dependence $R_h(\alpha)$ of the mean reflection coefficient is sensitive to structural defects of size $r_0 \sim 10$ nm and concentration $c \sim 10^{12}$–10^{13} cm^{-3}.

In the present paper we report systematic experimental results on DXS in crystals with microdefects obtained by the inclination method. In Sec. 2 we specialize the fundamental equations and results in the theory of DXS, first derived by Kato,[13,14] to the case of DXS in crystals with microdefects. Experimental values $R_{h,e}(\alpha)$ for the symmetric (220) Laue reflection for Si crystals with oxygen concentrations 10^{16}–10^{18} cm^{-3} are presented and discussed in Secs. 3 and 4, respectively.

2. THEORY OF DYNAMIC X-RAY SCATTERING IN CRYSTALS WITH RANDOMLY DISTRIBUTED MICRODEFECTS

Kato's statistical theory[13,14] of DXS in crystals with randomly distributed structural imperfections is based on the Takagi-Topen equations for the transmitted and diffracted wave amplitudes D_0, D_h:

$$\frac{\partial D_0}{\partial s_0} = i\sigma_{-h}\varphi(s_0, s_h) D_h(s_0, s_h),$$
$$\frac{\partial D_h}{\partial s_h} = i\sigma_h\varphi^*(s_0, s_h) D_0(s_0, s_h). \tag{2.1}$$

 0038-5646/87/030624-06$04.00

Here s_0, s_h are measured along the axes of the oblique coordinate system formed by the wave vectors of the transmitted and diffracted waves; the coefficients σ_{-h}, σ_h are related by

$$\sigma_{-h,h}=(\lambda C/\Omega)(e^2/mc^2)F_{-h,h}$$

to the structure factors F_{-h}, F_h for a perfect crystal lattice. Here Ω is the volume of the unit cell; the polarization factor C is equal to 1 for radiation polarized in the diffraction plane (s_0,s_h) and to $\cos 2\vartheta$ for radiation polarized in the plane perpendicular to it; $\Phi = \exp(i\mathbf{hu})$ depends exponentially on the displacement field $\mathbf{u}(s_0,s_h)$ of the crystal lattice sites caused by the defects.

Writing D_0, D_h, and φ in the form

$$D_{0,h}=\langle D_{0,h}\rangle+\partial D_{0,h}, \tag{2.2}$$

$$\varphi=\langle\varphi\rangle+\partial\varphi, \quad \langle\varphi\rangle=E \tag{2.3}$$

and neglecting correlations of order greater than two in the function φ, we get from (2.1) the following integrodifferential equations[13] for the mean amplitudes $\langle D_0\rangle$, $\langle D_h\rangle$:

$$\begin{aligned}\frac{\partial\langle D_0\rangle}{\partial s_0}&=i\sigma_{-h}E\langle D_h\rangle\\&\quad-\sigma^2\int_0^{s_h}\langle\partial\varphi(s_0,s_h)\,\partial\varphi^*(s_0,s_h-\eta)\rangle\langle D_0(s_0,s_h-\eta)\rangle\,d\eta,\\\frac{\partial\langle D_h\rangle}{\partial s_h}&=i\sigma_hE\langle D_0\rangle\\&\quad-\sigma^2\int_0^{s_0}\langle\partial\varphi^*(s_0-\xi,s_h)\,\partial\varphi(s_0,s_h)\rangle\langle D_0(s_0-\xi,s_h)\rangle\,d\xi.\end{aligned} \tag{2.4}$$

In general, these equations must be solved numerically. However, there is a class of problems of practical interest for which $\langle D_0\rangle$ and $\langle D_h\rangle$ in (2.4) vary slowly compared to the correlation function $g=(\langle\varphi\varphi^*\rangle-E^2)/(1-E^2)$. System (2.4) then reduces to a pair of differential equations of the form

$$\begin{aligned}\frac{\partial\langle D_0\rangle}{\partial s_0}&=i\sigma_{-h}E\langle D_h\rangle-\sigma^2(1-E^2)\tau\langle D_0\rangle,\\\frac{\partial\langle D_h\rangle}{\partial s_h}&=i\sigma_hE\langle D_0\rangle-\sigma^2(1-E^2)\tau\langle D_h\rangle,\end{aligned} \tag{2.5}$$

where

$$E=\langle\varphi\rangle \tag{2.6}$$

is the static Debye-Waller factor and

$$\tau=\int_0^\infty g(z)\,dz. \tag{2.7}$$

is the correlation length. The derivation of Eqs. (2.5) assumes that the correlation function $g(z)$ is isotropic.

Equations for the intensities $I^c_{0,h}=|\langle D_{0,h}\rangle|^2$ and $I^i_{0,h}=|\langle\partial D_{0,h}\rangle|^2$ of the coherent and diffuse components of the total intensities $I_{0,h}=I^c_{0,h}+I^i_{0,h}$ of the transmitted and diffracted waves can be derived by the same procedure used above to derive Eqs. (2.5) for the mean amplitudes from the Takagi-Topen equations (2.1) (see Ref. 13 for more details). When these equations are solved for the integrated intensity of the diffracted radiation for the case of symmetric Laue scattering (for which the normal $\mathbf{n}$ to the surface of the plane-parallel crystal is perpendicular to the diffraction vector $\mathbf{h}$), one obtains the expression[14]

$$R_h=R_h^c+R_h^i, \tag{2.8}$$

where the coherent component R^c_h of the intensity is given by

$$\begin{aligned}R_h^c&=H\exp\left[\left(-\frac{\mu\Lambda}{\pi\gamma}-\frac{2\pi(1-E^2)\gamma\tau}{\Lambda}\right)t\right]\\&\quad\times\left[\int_0^{2Et}J_0(x)\,dx+I_0(2E\varkappa t)-1\right],\end{aligned} \tag{2.9}$$

and the incoherent component R^i_h is

$$\begin{aligned}R_h^i&=H\exp\left[-\frac{\mu\Lambda}{\pi\gamma}t\right]\left[\frac{1-E^2}{2E}\right.\\&\left.+\frac{E^2(1-E^2)}{4}\frac{\pi\gamma\tau}{\Lambda^2}t^2\exp\left(-\frac{2\pi(1-E^2)\gamma\tau}{\Lambda}t\right)\right].\end{aligned} \tag{2.10}$$

Here $J_0(x)$ and $I_0(x)$ are the zero-order Bessel functions of real and imaginary argument, respectively; $\Lambda=\lambda/C|\chi_{hr}|$ is the extinction length; $t=\pi T/\Lambda\gg 1$ is the dimensionless crystal thickness; $\mu=2\pi\chi_{0i}/\lambda$ is the X-ray absorption coefficient; $H=\pi|\chi_{hr}|/2\sin 2\vartheta$ and $\varkappa=|\chi_{hi}|/|\chi_{hr}|$ are coefficients, where χ_{hr} and χ_{hi} are the real and imaginary parts of the Fourier component χ_h of the crystal polarizability; ϑ is the Bragg angle, and $\gamma=\cos\vartheta$.

Equations (2.9) and (2.10) show that the coherent and incoherent components R^c_h, R^i_h of the average intensity R_h depend differently on the crystal thickness—R^c_h oscillates with period Λ/E, while R^i_h decreases monotonically with t. Both are governed by two parameters, the static Debye-Waller factor and the correlation length τ, which describe how the crystal defects influence the dynamic X-ray scattering. The different thickness dependences can be exploited to solve the inverse DXS problem for crystals with microdefects, i.e., determine the parameters E and τ. Indeed, one can find E by using the inclination method to measure the oscillation period Λ/E of $R_h(t)$ (Refs. 15–17, see Sec. 3) and then calculate τ from Eqs. (2.8)–(2.10) and the general experimental dependence $R_h(\alpha)$ by a least-squares analysis.

3. EXPERIMENTAL METHOD AND RESULTS

In the inclination method (first proposed in Ref. 15) the DXS plane is inclined so that the diffraction is noncoplanar, as shown in Fig. 1. The ordinary expressions for the extinction and absorption lengths for Laue diffraction must be modified when the diffraction plane is inclined; for an asymmetric inclined configuration, we have

$$\Lambda_{\text{eff}}=\frac{(\cos^2\alpha\cos^2\psi\cos^2\vartheta-\sin^2\psi\sin^2\vartheta)^{1/2}}{\cos\vartheta}\Lambda, \tag{3.1}$$

$$\mu_{\text{eff}}=\frac{\cos\alpha\cos\psi\cos\vartheta}{\cos^2\alpha\cos^2\psi\cos^2\vartheta-\sin^2\psi\sin^2\vartheta}\mu. \tag{3.2}$$

Most experiments employ a symmetric configuration ($\psi=0$), which is particularly advantageous in our case (see below). Equations (3.1) and (3.2) then simplify, and

$$\Lambda_{\text{eff}}=(\cos\alpha)\Lambda, \tag{3.3}$$

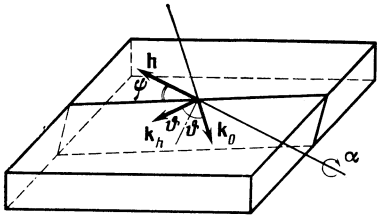

FIG. 1. Sketch of the inclination system for Laue diffraction.

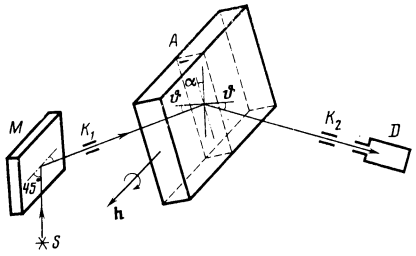

FIG. 3. Sketch of the experimental system.

which is equivalent to introducing an effective thickness

$$T_{\text{eff}}=T/\cos\alpha \qquad (3.4)$$

in the standard coplanar diffraction problem.

Expressions (3.1) and (3.3) for the extinction length Λ_{eff} can be interpreted physically as giving the beat length for two Bloch waves which are excited in the crystal during DXS of an incident plane wave satisfying Bragg's law. Figure 2 shows the projections of the two wave vectors on two mutually orthogonal planes for a symmetric DXS configuration.

Figure 3 shows the experimental configuration used to study DXS in crystals by the inclination method. The crystal A was mounted on a goniometer whose axis of rotation was normal to the reflecting planes of the crystal. The reflection conditions thus remained unchanged when the crystal was rotated about the goniometer axis. The X-ray diffraction measurement were carried out using σ-polarized Mo $K_{\alpha 1}$ radiation ($C=1$) for the (220) reflection from (100) single-crystal silicon plates. The primary X-ray beam was first polarized by reflecting it at the 44°40′ Bragg angle from an Fe–3% Si crystal in a monochromator (M); the emerging radiation was 99% σ-polarized. A collimating tube K_1 (Fig. 3) set the angular divergence of the beam incident on the crystal (S denotes the radiation source); the divergence was the same in both the vertical and the horizontal directions and was equal to 2′. A second collimator K_2 was used to decrease the background noise in the radiation reaching the detector D. A Philips "Norelko" diffractometer measured the curves $R_h(\alpha)$ automatically while the inclination angle α was incremented from $-40°$ to $+40$ °C in steps of 0.2°.

In the measurements we were careful to keep macroscopic elastic deformations of the crystal from distorting the mean DXS intensity. This was accomplished by using thick (~ 1 mm) single-crystal silicon plates whose sides were polished chemically and mechanically under identical conditions. In addition, $R_h(\alpha)$ was measured using a symmetric DXS configuration, for which only torques that "twist" the crystal plate can generate a deformation gradient capable of distorting the reflecting crystal planes. Distortions of the DXS by elastic macroscopic deformations can thus be neglected, since according to Ref. 11 the torgue in this case is an order of magnitude less than the bending moments, and measurements of the deformation in our crystals by the inclination method using the asymmetric (111) reflection yielded curves $R_{111}(\alpha)$ that were essentially identical to those for perfectly flat plates (the effective bending radius of the plates was at least 2000 m).

Figure 4 shows the experimentally recorded mean Laue reflection coefficient $R_h(\alpha)$ for the (220) reflection for silicon crystals with oxygen concentrations $c_{O2}=10^{16}$ cm^{-3} and $c_{O2}=10^{18}$ cm^{-3}. For crystals with $c_{O2}=10^{16}$ cm^{-3}, $R_{h,e}(\alpha)$ is nearly identical to $R_{h,id}(\alpha)$ (solid curve in Fig. 4a) calculated for a perfect crystal with $\Lambda_0=36.40\,\mu$m. The

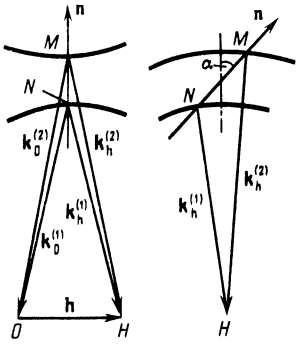

FIG. 2. Cross sections through the diffracting surface in two mutually perpendicular directions.

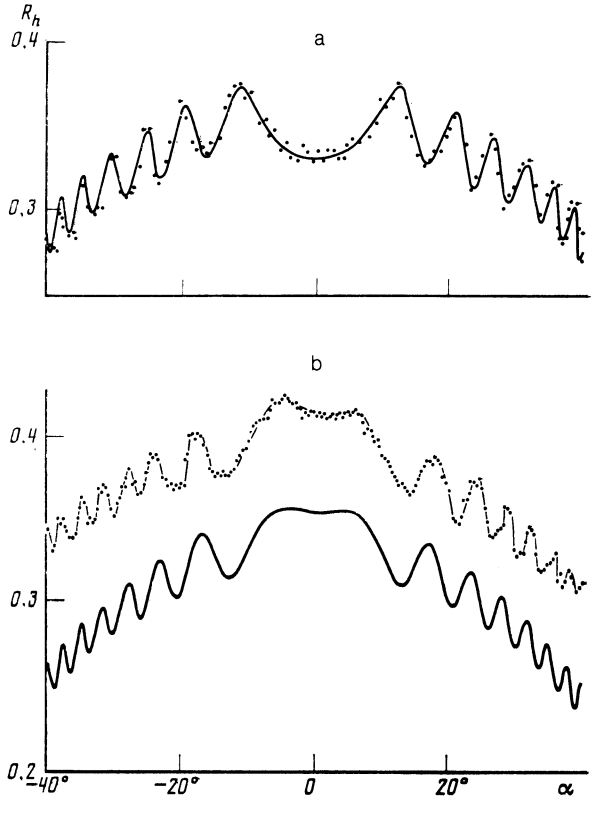

FIG. 4. Reflection coefficient $R_h(\alpha)$ for the (220) reflection from a silicon crystal: a) $c_{O2}=10^{16}$ cm^{-3}; b) $c_{O2}=10^{18}$ cm^{-3}; $R_h(\alpha)$ is normalized by $\overline{R}_h^0(\alpha)$, the corresponding value for a perfect nonabsorbing crystal.

period of the oscillations is somewhat greater for crystals grown by the Czochralski technique (Fig. 4b). According to Eqs. (2.8)–(2.10), this is because the extinction length for X-rays is greater by a factor of E^{-1} for crystals with randomly distributed microdefects. In other words, the effective extinction length is $\Lambda = \Lambda_0/E$ and hence the static Debye-Waller factor E can be found from the oscillation period of the experimental curve $R_{h,e}(\alpha)$. Since E is nearly equal to unity, it is important to consider the error incurred in deducing it from $R_{h,e}(\alpha)$.

The following procedure was used to find the mean extinction length $\bar{\Lambda}$ and its variance $\sigma^2(\bar{\Lambda})$ from the experimental data $R_{h,e}(\alpha)$ and the formulas (2.8)–(2.10). The extinction lengths Λ_i where calculated for the inclination angles α_i at which the oscillations in $R^c_{h,e}(\alpha)$ vanished, because the error $\delta\alpha_i = \delta R_{h,i}(\partial R_h/\partial\alpha_i)^{-1}$ in measuring the position of the ith oscillation is least at these points for a fixed mesurement error $\delta R_{h,i}$ (in our case $\delta R_{h,i}$ was $\sim 0.05\, R_{h,i}$). The values Λ_i where then analyzed by the least-squares method (see, e.g., Ref. 18), and $\bar{\Lambda}$ and $\sigma^2(\bar{\Lambda})$ were computed by the formulas

$$\bar{\Lambda} = \Big(\sum_i\sum_j \Lambda_i D_{ij}^{-1}\Lambda_j\Big)\Big(\sum_i\sum_j D_{ij}^{-1}\Big)^{-1}, \tag{3.5}$$

$$\sigma^2(\bar{\Lambda}) = \Big[\sum_i\sum_j (\Lambda_i-\bar{\Lambda})D_{ij}^{-1}(\Lambda_j-\bar{\Lambda})\Big] \times \Big[(n-1)\sum_i\sum_j D_{ij}^{-1}\Big]^{-1}, \tag{3.6}$$

where D_{ij}^{-1} are the components of the weight matrix D^{-1} inverse to the error matrix

$$D = \begin{pmatrix} \sigma^2(\Lambda_1) & \operatorname{cov}(\Lambda_1,\Lambda_2) & \dots \operatorname{cov}(\Lambda_1,\Lambda_n) \\ \operatorname{cov}(\Lambda_1,\Lambda_2) & \sigma^2(\Lambda_2) & \dots \operatorname{cov}(\Lambda_2,\Lambda_n) \\ \dots & \dots & \dots \\ \operatorname{cov}(\Lambda_1,\Lambda_n) & \operatorname{cov}(\Lambda_2,\Lambda_n)\dots & \sigma^2(\Lambda_n) \end{pmatrix}. \tag{3.7}$$

The error $\delta\Lambda_i$ in Λ_i at the point $\alpha = \alpha_i$ on the measured curve $R_{h,e}(\alpha)$ is given by

$$\delta\Lambda_i = \Lambda_i[(\delta T/T)^2 + (\operatorname{tg}\alpha_i\delta\alpha_i)^2]^{1/2}, \tag{3.8}$$

where we have used the fact that the errors in measuring $R_{h,i}$ and the crystal thickness T are statistically independent. The terms

$$\operatorname{cov}(\Lambda_j,\Lambda_j) = \Lambda_i\Lambda_j(\delta T/T)^2 \tag{3.9}$$

are present due to systematic errors in measuring T, which cause the errors in Λ_i and Λ_j at the two angles α_i and α_j to be mutually correlated. We observe that because the errors in the extinction lengths Λ_i are not statistically independent [$\operatorname{cov}(\Lambda_i,\Lambda_j)\neq 0$], the variance $\sigma^2(\bar{\Lambda})$ can easily be shown to satisfy the inequality

$$\sigma^2(\bar{\Lambda})/\bar{\Lambda}^2 > (\delta T)^2/T^2, \tag{3.10}$$

i.e., the relative error in determining $\bar{\Lambda}$ is greater than the error in measuring the crystal thickness, regardless of the total number of measurements n.

Table I lists the extinction lengths $\bar{\Lambda}$ found from the expeirmental data $R_{h,e}(\alpha)$ shown in Fig. 4. For comparison, some extinction lengths and atomic scattering amplitudes found previously by other methods are also given.

The second parameter in the DXS theory, the correlation length τ, can be calcualted similarly. Here it is convenient to use the nonoscillating component (averaged over an oscillation period) of the mean reflection coefficient $\bar{R}_{h,e}(\alpha)$. For each α_k, the corresponding τ_k is found by requiring that $|\bar{R}_{h,k} - \bar{R}_h(\alpha_k,\tau_k)| \leqslant 0.03\,\bar{R}_{h,k}$. The error in τ_k, the mean correlation length $\bar{\tau}$, and the variance $\sigma^2(\bar{\tau})$ were computed by the formulas

$$\delta\tau_k = \Big\{(\delta\bar{R}_{h,k})^2 \Big/ \Big(\frac{\partial\bar{R}_h}{\partial\tau}\Big|_{\alpha_k,\tau_k}\Big)^2 + \Big(\frac{\partial\bar{R}_h}{\partial E}\Big|_{\alpha_k,\tau_k}\Big)^2(\delta E)^2 \Big/ \Big(\frac{\partial\bar{R}_h}{\partial\tau}\Big|_{\alpha_k,\tau_k}\Big)^2\Big\}^{1/2}, \tag{3.11}$$

$$\bar{\tau} = \Big[\sum_k \frac{\tau_k}{\sigma^2(\tau_k)}\Big]\Big[\sum_k \frac{1}{\sigma^2(\tau_k)}\Big]^{-1}, \tag{3.12}$$

$$\sigma^2(\bar{\tau}) = \Big[\sum_k \frac{(\tau_k-\bar{\tau})^2}{\sigma^2(\tau_k)}\Big]\Big[(m-1)\sum_k \frac{1}{\sigma^2(\tau_k)}\Big]^{-1}. \tag{3.13}$$

The calculated results were used to find $\tau(\alpha)$, which is shown in Fig. 5. We see that τ lies between 5 and 13 nm, which corresponds to microdefects with a mean radius of 3–10 nm (see below). It should be noted that the dependence of τ on the angle α is inconsistent with the assumed isotropy of the correlation function $g(z)$ (see Sec. 2), i.e., the displacement fields caused by the microdefects are anisotropic. However, since we seek only qualitative information regarding the crystal defect structure and confine ourseleves to order-of-magnitude estimates of the concentration and mean size of the defects, we may without loss of generality take the

TABLE I. Extinction lengths and atomic scattering amplitudes for silicon crystals [(220) reflection of σ-polarized Mo K_α radiation].

Crystal properties and method of study	Extinction length, μm	Atomic scattering amplitude	Static factor
$c_{O_2}=10^{16}$ cm^{-3} $T=804\pm1$ μm	36.39±0.03	8.500±0.007	1
$T=794\pm1$ μm	36.40±0.04	8.497±0.009	1
$c_{O_2}=10^{18}$ cm^{-3} $T=848\pm1$ μm	36.56±0.05	8.460±0.011	0.996±0.0015
$T=838.5\pm1$ μm	36.54±0.05	8.465±0.011	0.996±0.0015
By measuring the intensities in the Debye pattern[19]	36.47±0.08	8.48±0.02	–
By sectional topography	36.04±0.38	8.58±0.09	–
	36.48±0.034	8.478±0.008	–
Inclination method[15]	36.58±0.02	8.456±0.005	–

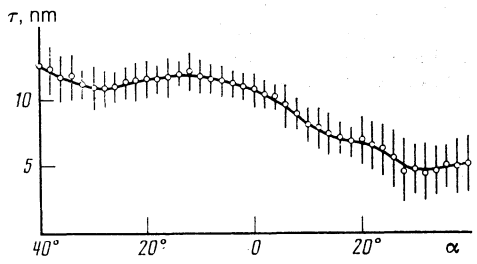

FIG. 5. Correlation length τ versus inclination angle α for the (220) reflection from a silicon crystal with $c_{O2} = 10^{18}$ cm^{-3}.

correlation length τ to be constant and equal to its mean value $\bar{\tau} = 9$ nm (see (3.12)).

4. DISCUSSION

We use the simple model proposed previously in Ref. 22 to relate the empirically determined static Debye-Waller factor E and correlation length τ (Sec. 3) to the physical characteristics of the crystal defect structure. The model assumes that the defects are uniformly distributed isotropic inclusions of radius r_0, and the elastic displacement field associated with each inclusion is given by the familiar expression (see, e.g., Ref. 23)

$$\begin{aligned} \mathbf{u}(\mathbf{r}) &= \varepsilon \mathbf{r}, \quad |\mathbf{r}| \leqslant r_0, \\ \mathbf{u}(\mathbf{r}) &= \varepsilon r_0 \mathbf{r}/|\mathbf{r}|^3, \quad |\mathbf{r}| \geqslant r_0, \end{aligned} \tag{4.1}$$

where the mismatch parameter ε is equal to 0.02 for silicon.

The correlation function $g(\eta)$ can be written in the form[22]

$$g(\eta) = (e^{-T(\eta)} - E^2)/(1-E^2), \tag{4.2}$$

where the function $T(\eta)$, which was introduced by Krivoglazov, is given by

$$T(\eta) = c \int_V [1 - e^{i\mathbf{h}\mathbf{u}(\mathbf{r})} e^{-i\mathbf{h}\mathbf{u}(\mathbf{r}+\eta)}]\, d\mathbf{r} \tag{4.3}$$

for $c\Omega \ll 1$ (the integration is over the volume of the crystal).

The static Debye-Waller factor is given in terms of $T(\infty)$ by

$$E = e^{-M}, \tag{4.4}$$

where

$$M = c \int_V [1 - e^{i\mathbf{h}\mathbf{u}(\mathbf{r})}]\, d\mathbf{r}. \tag{4.5}$$

Expanding the exponentials in (4.3), (4.5) in powers of $\mathbf{h}\cdot\mathbf{u} \ll 1$ and keeping only the lowest-order nonvanishing terms, we find after a straightforward calculation that

$$g(\eta) = \left(\frac{5}{4}\frac{r_0}{\eta} - \frac{1}{2}\frac{r_0^3}{\eta^3}\right)\sin^2\vartheta + \frac{r_0^3}{\eta^3}\cos^2\vartheta, \quad \eta \geqslant 2r_0, \tag{4.6}$$

$$g(\eta) = 1 - \left(\frac{\eta^2}{4r_0^2} - \frac{5}{64}\frac{\eta^3}{r_0^3} + \frac{\eta^5}{512 r_0^5}\right) \times \sin^2\vartheta - \left(\frac{\eta^2}{3r_0^2} - \frac{11}{718}\frac{\eta^5}{r_0^5}\right)\cos^2\vartheta, \quad \eta \leqslant 2r_0,$$

$$M = {}^8/_5 \pi c \varepsilon^2 h^2 r_0^5. \tag{4.7}$$

In deriving (4.6) we have assumed that $1 - E^2 \ll 1$.

The function $g(\eta)$ is shown in Fig. 6. It is noteworthy that according to Eq. (4.6) the integral

$$\int_0^\infty g(\eta)\, d\eta,$$

which by (2.7) determines the correlation length τ, diverges logarithmically at the upper limit. However, physical considerations show that the upper limit in (2.7) is actually finite—it must be much greater than the radius of the defects and much smaller than the extinction length Λ. We thus get our final estimates

$$c = 5(1-E^2)/8\pi\varepsilon^2 h^2 r_0^5, \quad r_0 = (0.5-0.8)\bar{\tau} \tag{4.8}$$

for the defect concentration and radius from Eqs. (4.6), (4.7). The values are $c \sim 10^{13}$ cm^{-3} and $r_0 \sim 7$ nm for a silicon crystal with oxygen concentration 10^{18} cm^{-3} under our experimental conditions.

Our studies thus show that small defects present in low concentrations can alter dynamic X-ray scattering in crystals. X-ray diffraction data obtained by the inclination method can be used to find the static Debye-Waller factor and the correlation function for the random elastic displacements of the atoms in the crystal lattice and thereby gain insight into the defect structure in the crystal.

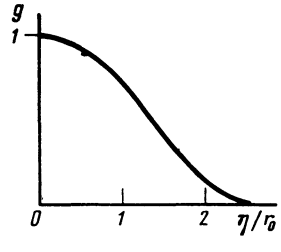

FIG. 6. Correlation function for the (220) reflection of σ-polarized Mo $K_{\alpha 1}$ radiation from a silicon crystal containing uniformly distributed isotropic inclusions of radius r_0.

[1] A. M. Elistratov and O. N. Efimov, Fiz. Tverd. Tela **4**, 2397 (1962) [Sov. Phys. Solid State **4**, 1757 (1963)].
[2] A. M. Elistratov and O. N. Efimov, Fiz. Tverd. Tela **5**, 1869 (1963) [Sov. Phys. Solid State **5**, 1304 (1964)].
[3] S. Maruyama, J. Phys. Soc. Jpn. **20**, 1399 (1965).
[4] O. N. Efimov, E. F. Sheikhet, and L. I. Datsenco, Phys. Status Solidi **38**, 489 (1970).
[5] A. Iida and K. Kohra, Phys. Status Solidi. (a) **51**, 533 (1979).
[6] A. M. Afanas'ev, M. V. Koval'chuk, É. F. Lobanovich, *et al.*, Kristallogr. **26**, 28 (1981) [Sov. Phys. Crystallogr. **26**, 13 (1981)].
[7] P. Zaumseil and U. Winter, Phys. Status Solidi (a) **73**, 455 (1982).
[8] V. B. Molodkin, S. I. Olikhovskiĭ, M. E. Osinovskiĭ, *et al.*, Metallofiz. **6**, No. 3, 7 (1984).
[9] P. V. Petrashen', Metallofiz. **8**, No. 1, 35 (1986).
[10] P. V. Petrashen' and F. N. Chukhovskiĭ, Metallofiz. **8**, No. 3, 45 (1986).
[11] S. N. Voronkov, S. K. Maksimov, and F. N. Chukhovskiĭ, Fiz. Tverd. Tela **26**, 2019 (1984) [Sov. Phys. Solid State **26**, 1225 (1984)].
[12] P. V. Petrashen' and F. N. Chukhovskiĭ, Zh. Eksp. Teor. Fiz. **69**, 477 (1975) [Sov. Phys. JETP **42**, 243 (1975)].
[13] N. Kato, Acta Crystallogr. A **36**, 763 (1980).
[14] N. Kato, Acta Crystallogr. A **36**. 770 (1980).
[15] K. Utemisov, V. P. Somenkova, V. A. Somenkov, and S. Sh. Shil'shteĭn, Kristallogr. **25**, 845 (1980) [Sov. Phys. Crystallogr. **25**, (1980)].
[16] N. M. Olekhnovich, A. L. Karpei, A. I. Olekhnovich, and L. D. Puzenkova, Acta Crystallogr. A **39**, 116 (1983).
[17] N. M. Olekhnovich and A. L. Karpei, Phys. Status Solidi (a) **82**, 365 (1984).

[18]D. J. Hudson, Lectures on Elementary Statistics and Probability, CERN Report CERN 63-29 (Aug. 1963), *continued as* Statistics Lectures II: Maxiumum Likelihood and Least Squares Theory, CERN Report CERN 64-18 (April 1964).
[19]S. Göttlicher and E. Wölfel, Z. Electrochem. **63**, 891 (1959).
[20]H. Hattory, H. Kuriyama, T. Katagawa, and N. Kato, J. Phys. Soc. Jpn. **20**, 988 (1965).
[21]M. Hart and A. Milne, Acta Crystallogr. A **25**, 134 (1975).
[22]S. N. Voronkov, F. N. Chukhovskiĭ, and D. I. Piskunov, Fiz. Tverd. Tela **27**, 1911 (1985) [Sov. Phys. Solid State **27**, 1151 (1985)].
[23]M. A. Krivoglaz, Diffraktsiya Rentgenovskikh Lucheĭ i Neĭtronov v Neideal'nykh Kristallakh (X-ray and Neutron Diffractionin in Imperfect Crystals), Naukova Dumka, Kiev (1983).

Translated by A. Mason